Article

Non-Aqueous Solvent Mixtures for CO$_2$ Capture: Choline Hydroxide-Based Deep Eutectic Solvents Absorbent Performance at Various Temperatures and Pressures

Mohd Azlan Kassim [1,*], **Nor Afifah Sulaiman** [1], **Rozita Yusoff** [2] **and Mohamed Kheireddine Aroua** [1,3,4]

[1] Research Centre for Carbon Dioxide Capture and Utilisation (CCDCU), School of Engineering and Technology, Sunway University, No. 5 Jalan Universiti, Bandar Sunway, Petaling Jaya 47500, Selangor, Malaysia; afifahsulaiman55@gmail.com (N.A.S.); kheireddinea@sunway.edu.my (M.K.A.)
[2] Chemical Engineering Department, Faculty of Engineering, University of Malaya, Kuala Lumpur 50603, Malaysia; ryusoff@um.edu.my
[3] School of Engineering, Lancaster University, Lancaster LA1 4YW, UK
[4] Sunway Materials Smart Science & Engineering Research Cluster (SMS2E), Sunway University, No. 5 Jalan Universiti, Bandar Sunway, Petaling Jaya 47500, Selangor, Malaysia
* Correspondence: azlanka@sunway.edu.my; Tel.: +60-0374918622 (ext. 7627)

Abstract: Carbon dioxide (CO$_2$) absorption in a non-aqueous solution is a potential technology for reducing greenhouse gas emissions. In this study, a non-aqueous solvent, sulfolane and dimethyl-sulfoxide (DMSO), was functionalized with a deep eutectic solvent (DES) consisting of choline hydroxide and polyamines diethylenetriamine (DETA) and triethylenetetramine (TETA). The non-aqueous absorbents' CO$_2$ absorption ability was investigated in a high-pressure absorption reactor with a variable absorption temperature (303.15–333.15 K) and pressure (350–1400 kPa). The results showed that 2M ChOH:TETA−DMSO solution had the highest CO$_2$ loading capacity when compared with other screened solutions, such as 2M ChOH:TETA−Sulfolane, 2M ChOH:DETA−DMSO and 2M ChOH:DETA−Sulfolane. It was also found that the absorption capacity increased with increasing pressure and decreased with temperature. The highest CO$_2$ absorption by 2M ChOH:TETA−DMSO was observed at a partial pressure of 1400 kPa at 303.15 K 1.2507 mol CO$_2$/mol DES. The use of a non-aqueous solvent in the mixture showed a phase separation phenomenon after the CO$_2$ absorption reaction due to the formation of insoluble carbamate salt, which was identified through FTIR analysis. These findings suggest that the use of a DES polyamine mixed with a non-aqueous solvent could be a promising solution for CO$_2$ capture.

Keywords: deep eutectic solvent; polyamine; CO$_2$ absorption; non-aqueous

1. Introduction

Among the primary pollutant acid gases, CO$_2$ is considered the most significant, as it contributes to around 77% of greenhouse gases leading to global warming. CO$_2$ emissions can be controlled by separating CO$_2$ from the gaseous streams in natural treatment plants or flue gas from industrial plants. Post-combustion CO$_2$ capture processes are currently one of the most common technologies used in experimental laboratories and industrial applications. Absorption, adsorption, membrane separation and cryogenic separation are the most commonly used techniques in post-combustion capture technology. According to the literature, the absorption process has been widely used in comparison to other separation techniques, particularly in the oil and gas sector, coal power plants, and the chemical industry [1,2]. This is mainly because of its dependable technology, vast processing capacity, and long history of industrial operation [3,4]. Traditionally, organic solvents are the most widely used in these applications. The first commercial solvent used in gas purification was triethanolamine (TEA), followed by monoethanolamine (MEA) and diethanolamine (DEA). The problem with organic solvents is that they are extremely

reactive and cytotoxic, with a high regeneration cost, equipment corrosion, and oxidative degradation for some amines [5,6]. The high volatility of aqueous amine solutions results in increased regeneration energy requirements. Hence, nonvolatile ionic liquids were introduced to overcome this problem. As a result, the present concept of employing deep-eutectic ionic liquids (DES) is gaining attraction because of their low cost, simple production processes, low volatility, biodegradability, and non-toxicity [7,8]. Figure 1 shows the number of publications on DES for CO_2 absorption from 2014–2022. In recent years, researchers have synthesized DES by mixing hydrogen bond acceptors (HBA) and hydrogen bond donors (HBD). Abbott and colleagues studied and reported the first DES system in 2003, which comprised quaternary ammonium salt choline chloride (ChCl) and urea in the molar ratio of 1:2. A study by Leron and Li (2013) on the synthesis of choline chloride: ethylene glycol with a 1:2 molar ratio shows a high CO_2 absorption capacity at 3.126 mol/mol DES [9]. Another study by Ali et al. (2014), whereby they synthesized a 1:2.5 molar ratio of choline chloride:urea, recorded a CO_2 uptake of up to 0.0211 mol/mol DES [10]. According to Mahi et al. (2019), non-aqueous solvents could be a solution for CO_2 absorption [11]. In their work, 30% MEA was combined with choline chloride:ethylene glycol in a 1:2 molar ratio. The CO_2 absorption shows 0.8 mol/mol DES being absorbed in the solution.
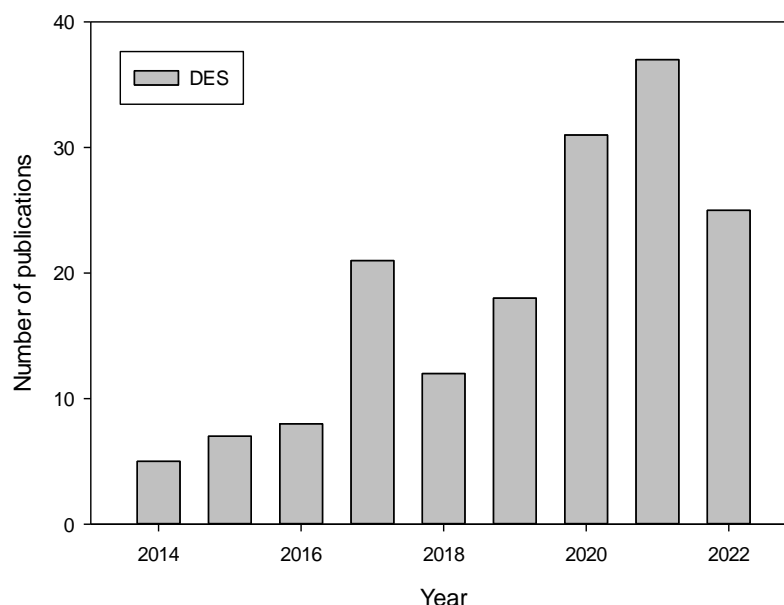
Figure 1. DES publications for CO_2 removal from 2014–2022.

In the present work, we synthesized DES by mixing an equimolar ratio of choline hydroxide (ChOH) as HBA with diethylenetriamine (DETA) and triethylenetetramine (TETA) as HBD to introduce mixtures of DES non-aqueous solvent. These solvents are gaining attention as energy-saving solvents that efficiently absorb CO_2 with a significant reduction in regeneration energy costs due to the absence of water [12,13]. Dimethylsulfoxide (DMSO) and sulfolane were chosen as the non-aqueous solvents in this study. DMSO can dissolve aromatic, unsaturated hydrocarbons and many inorganic salts, which makes DMSO a powerful and versatile physical solvent [14]. A current study reported that DMSO was used as a diluent not only to reduce energy consumption due to low vaporization energy and low heat capacity but also due to being a non-corrosive organic solvent [13,15,16]. On the other hand, sulfolane was chosen due to its maturity in acid gas removal processes [17]. There is a wide range of studies regarding the use of sulfolane as a promising non-volatile organic solvent with low corrosivity and exceptional solubility, which could potentially improve CO_2 absorption capability [18,19].

2. Materials and Methods

2.1. Materials

The following are the raw materials used in polyamine synthesis. DETA, TETA, choline chloride, 45% in methanol, sulfolane and DMSO were purchased from Sigma-Aldrich (M) Sdn. Bhd., Petaling Jaya, Malaysia. All products were used without further purifications with a high purity, as summarized in Table 1.

Table 1. Table of provenance for the compound system.

Chemicals	CASRN	Source	Purity
45% Choline hydroxide in methanol	123-41-1	Sigma-Aldrich	99%
DETA	111-40-0	Merck	98%
TETA	112-24-3	Merck	98%
Carbon dioxide	MY 006-474	Alpha Gas Solution	99%
Sulfolane	126-33-0	Aldrich	99%
DMSO	67-68-5	Sigma-Aldrich	99%

2.2. Synthesis of DES

ChOH:TETA and ChOH:DETA were synthesized according to the literature [20]. An equimolar mixture of 45 wt% ChOH in methanol and polyamines (DETA, TETA) was mixed in a round bottom flask with heating and stirring at 353.15 K for 30 min. Then, the solvent removal took place in a rotary evaporator for 2 h under reduced pressure. The sample was then dried in a vacuum oven overnight with 70 mbar pressure to remove excess moisture, and the acquired DES was obtained and kept in tightly sealed bottles.

2.3. Sample Preparation

The components were weighed using a calibrated single pan digital balance (HR-250AZ, A&D Limited, Toshima, Japan) with an accuracy of 0.1 mg to make 2M DES non-aqueous mixtures. To reduce moisture absorption from the environment, all mixes were maintained in tightly sealed bottles.
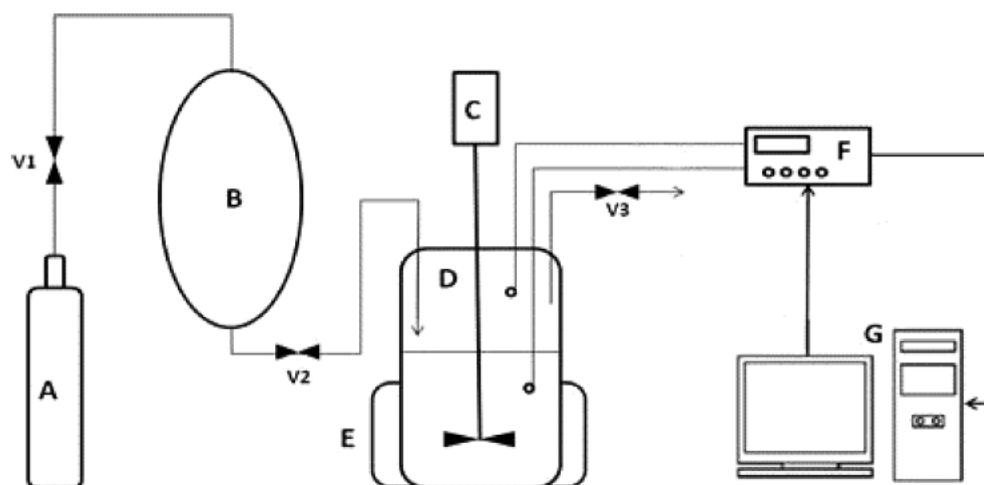
2.4. CO_2 Solubility Measurements

The solubility of CO_2 was determined using a pressure drop method, as previously reported. Figure 2 depicts a schematic of the experimental setup, which includes a welded stirrer assembly, a thermocouple, an intake gas tube, and an air vent. Both integrated reactors were outfitted with a thermostat heater and a thermocouple. To begin the experiment, the system was purged with air by flushing it with CO_2. Next, purified CO_2 from a gas tank was introduced and heated to the desired temperature. A high-pressure reactor cell holding 20 mL of 2M DES mixtures was sealed, and CO_2 gas was continually supplied, while the sample was agitated until equilibrium was achieved. The pressure in the system gradually decreased, and equilibrium was achieved once the pressure in the reactor cell remained constant.

The amount of CO_2 in the gas phase was calculated using the known volume, pressure, and temperature parameters. The initial and final pressures (equilibrium pressure) that were previously recorded were used to calculate the mole differences during the absorption process. The CO_2 solubility was calculated from the modified Ideal Gas Law to accurately estimate the number of moles of CO_2 absorbed, as expressed in Equation (1) [21],

$$\chi = \frac{\left[\frac{(P_{Ti}-P_{Vi}) \times V_{gc}}{zRT}\right] - \left[\frac{(P_{Tf}-P_{Vf}) \times (V_{gc}+(V_{cell}-V_{sol}))}{zRT}\right]}{n_{total}} \tag{1}$$

where χ is the CO_2 loading in mol of CO_2/total mol of DES. P_T is the total pressure (kPa), P_V is the vapor pressure, V_{gc} is the volume of the gas container, V_{cell} is the volume of the

reactor cell, V_{sol} is the volume of the solution, i is the initial condition, and f is the final condition. Meanwhile, n_{total} is the summation of the moles of DES in the liquid phase.

Figure 2. Schematic diagram of the experimental set-up for measuring the CO_2 solubility: A. Gas (CO_2) cylinder; B. Gas (CO_2) reservoir; C. Motor; D. High-pressure reactor vessel (equilibrium cell); E. Heater; F. Reactor controller; G. PC graphical user interface; V1. Control valve; V2. Needle valve; V3. Pressure relief valve.

2.5. Apparatus Validation

In order to evaluate the consistency of the equipment, an apparatus reliability study was performed, and the results were compared to those found in the previously reported data by Jalili et al. (2015) [22]. A series of runs were conducted at various pressures using sulfolane at a temperature of 303.15 K. The data obtained were compared to literature values, as depicted in Figure 3, and yielded an average absolute relative deviation (AARD) of 0.461%.
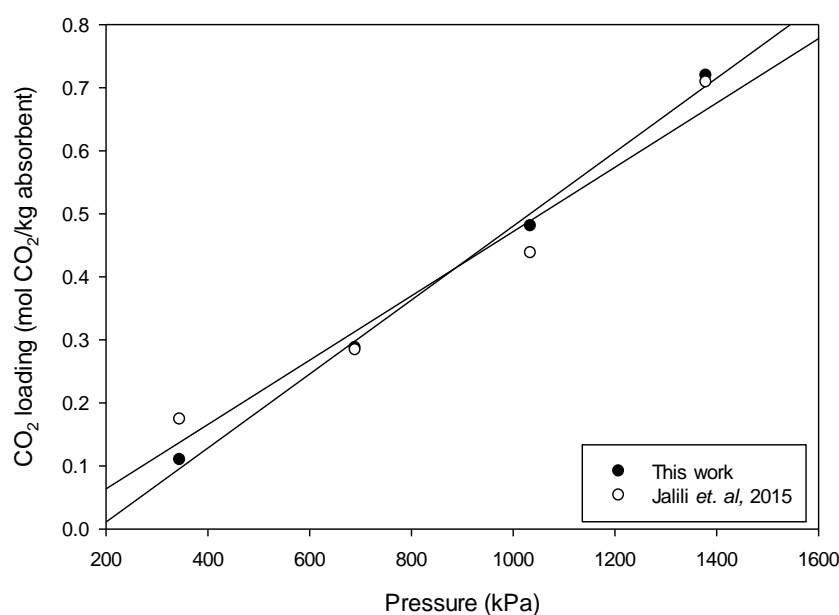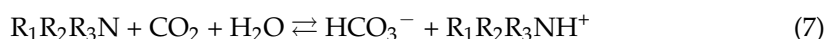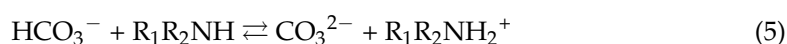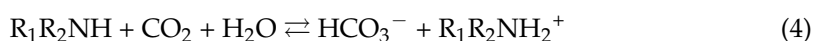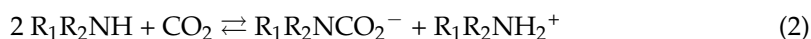

Figure 3. Comparison of measured CO_2 loading in sulfolane with literature [22] at 303.15 K.
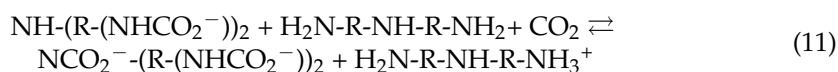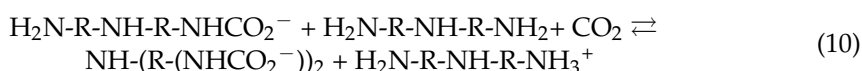
3. Results and Discussion

3.1. Chemical Equilibria

The chemical route between polyamine and CO_2 is quite complicated, as each of a polyamine molecule's amine moieties can interact with CO_2 individually. In both aqueous

and organic solvents, primary and secondary amine groups (denoted as R_1R_2H, with $R_1 = H$ for primary amines) engage in the primary reaction pathway, resulting in the creation of the matching amine carbamate ($R_1R_2NCO_2^-$) species. Aqueous solutions, on the other hand, produce bicarbonate and carbonate products. In aqueous environments, tertiary amine functionality ($R_1R_2R_3N$) reacts with CO_2 to produce bicarbonate (Equation (7)), but it is unable to form carbamate (Equation (2)) due to the absence of hydrogen atoms [23].

$$2\ R_1R_2NH + CO_2 \rightleftarrows R_1R_2NCO_2^- + R_1R_2NH_2^+ \tag{2}$$

$$R_1R_2NCO_2^- + CO_2 + 2\ H_2O \rightleftarrows 2\ HCO_3^- + R_1R_2NH_2^+ \tag{3}$$

$$R_1R_2NH + CO_2 + H_2O \rightleftarrows HCO_3^- + R_1R_2NH_2^+ \tag{4}$$

$$HCO_3^- + R_1R_2NH \rightleftarrows CO_3^{2-} + R_1R_2NH_2^+ \tag{5}$$

$$CO_2 + CO_3^{2-} + H_2O \rightleftarrows 2\ HCO_3^- \tag{6}$$

$$R_1R_2R_3N + CO_2 + H_2O \rightleftarrows HCO_3^- + R_1R_2R_3NH^+ \tag{7}$$

Polycarbamate species can occur when two or more amino functionalities of a polyamine experience simultaneous chemical reactions. As a result, polyamines with primary and secondary functionalities can form polycarbamate compounds via the following reaction between a carbamate and CO_2, as shown in Equations (8)–(11), where $H_2N–R–NH–R–NH_2$ stands for a generic triamine with two primary amino groups and a singular secondary group [24].

$$H_2N\text{-}R\text{-}NH\text{-}R\text{-}NH_2 + CO_2 \rightleftarrows {}^+H_3N\text{-}R\text{-}NH\text{-}R\text{-}NHCO_2^- \tag{8}$$

$$2\ H_2N\text{-}R\text{-}NH\text{-}R\text{-}NH_2 + CO_2 \rightleftarrows H_2N\text{-}R\text{-}NH\text{-}R\text{-}NHCO_2^- + H_2N\text{-}R\text{-}NH\text{-}R\text{-}NH_3^+ \tag{9}$$

$$\begin{aligned} H_2N\text{-}R\text{-}NH\text{-}R\text{-}NHCO_2^- + H_2N\text{-}R\text{-}NH\text{-}R\text{-}NH_2 + CO_2 \rightleftarrows \\ NH\text{-}(R\text{-}(NHCO_2^-))_2 + H_2N\text{-}R\text{-}NH\text{-}R\text{-}NH_3^+ \end{aligned} \tag{10}$$

$$\begin{aligned} NH\text{-}(R\text{-}(NHCO_2^-))_2 + H_2N\text{-}R\text{-}NH\text{-}R\text{-}NH_2 + CO_2 \rightleftarrows \\ NCO_2^-\text{-}(R\text{-}(NHCO_2^-))_2 + H_2N\text{-}R\text{-}NH\text{-}R\text{-}NH_3^+ \end{aligned} \tag{11}$$

3.2. CO₂ Absorption of 2M DES in Non-Aqueous Solutions

Figure 4a–d illustrates the solubility data for CO_2 in 2M DES non-aqueous mixtures measured experimentally. The equilibrium exhibits a typical pattern in which the CO_2 loading decreases with an increasing temperature and increases with an increasing pressure. Each combination in the figures shows a decreasing trend with rising temperatures from 303.15 to 333.15 K, demonstrating a high loading of CO_2 at lower temperatures at a constant pressure. The observed behaviors can be explained by a rise in the vapor pressure with the temperature, which results in a decrease in CO_2 loading. At a constant temperature, however, a rise in pressure has a positive influence on CO_2 solubility. This phenomenon may be described by the direct relation between gas diffusion into liquid and gas pressure above the solution's surface. In correlation with this study, the phenomenon could be seen in most of the DES non-aqueous mixtures, except for DES that contains DETA, where a high gas solubility could be seen at 313.15 K. A recent study by Tzirakis and coworkers reported that the highest CO_2 absorption was observed at 313.15 K with 1.68 mol/mol [25]. Another

study by Lua and team found that the CO_2 absorption capacity of the DETA mixture was the highest at 313.15 K with 1.70 mol/mol [26].

From the observations, it can be noted that, at the highest measured pressure, the 2M ChOH:TETA−DMSO mixture had the highest CO_2 absorption capacity, while the 2M ChOH:DETA−Sulfolane mixture had the lowest CO_2 absorption capacity among the mixtures. In general, the trend of CO_2 uptake is as follows: 2M ChOH:TETA−DMSO > 2M ChOH:TETA−Sulfolane > 2M ChOH:DETA−DMSO > 2M ChOH:DETA−Sulfolane. Moreover, the results of this work showed that the CO_2 absorption capacity was reduced at elevated temperatures, which agrees with the findings of the literature. For example, at 303.15 K and 1400 kPa, the CO_2 solubility of 2M ChOH:TETA−DMSO was 1.251 mol CO_2/mol DES and was reduced to 0.7566 mol/mol at a 333.15 K temperature.
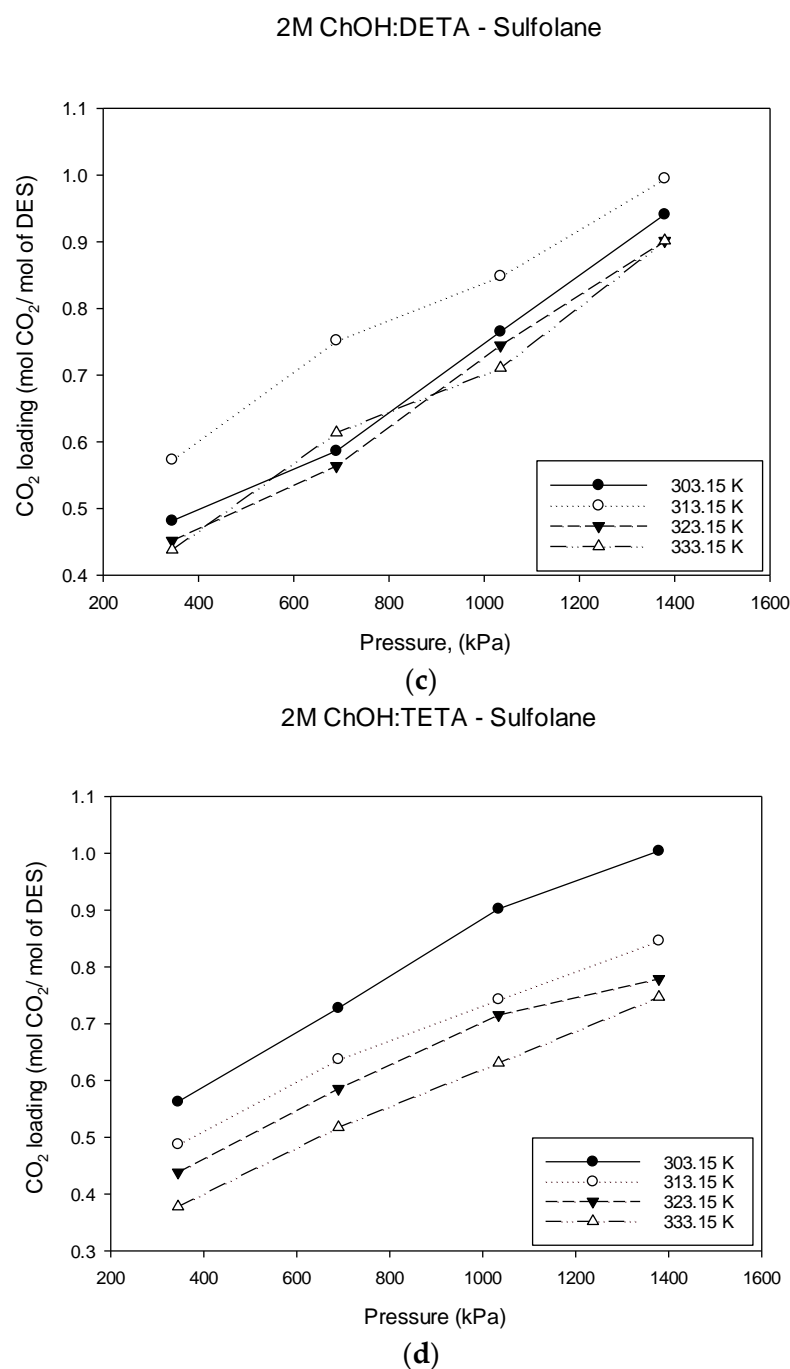
2M DETA:ChOH - DMSO

(**a**)
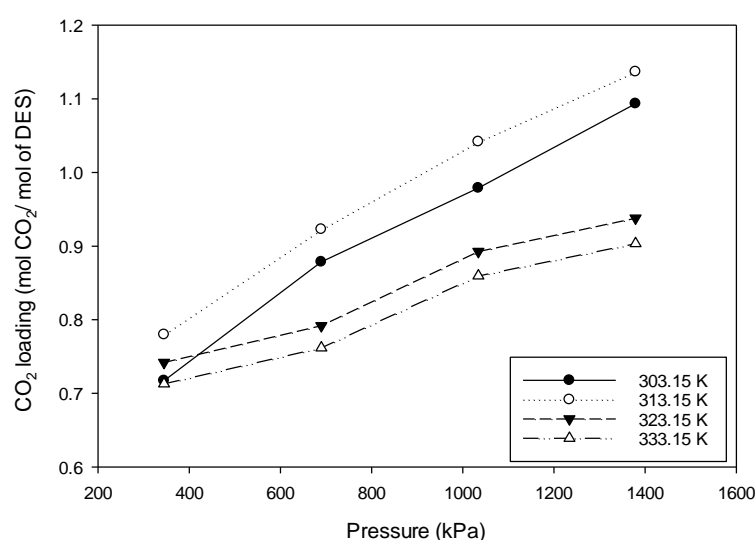
2M ChOH:TETA - DMSO

(**b**)

Figure 4. *Cont.*

2M ChOH:DETA - Sulfolane

(**c**)

2M ChOH:TETA - Sulfolane

(**d**)
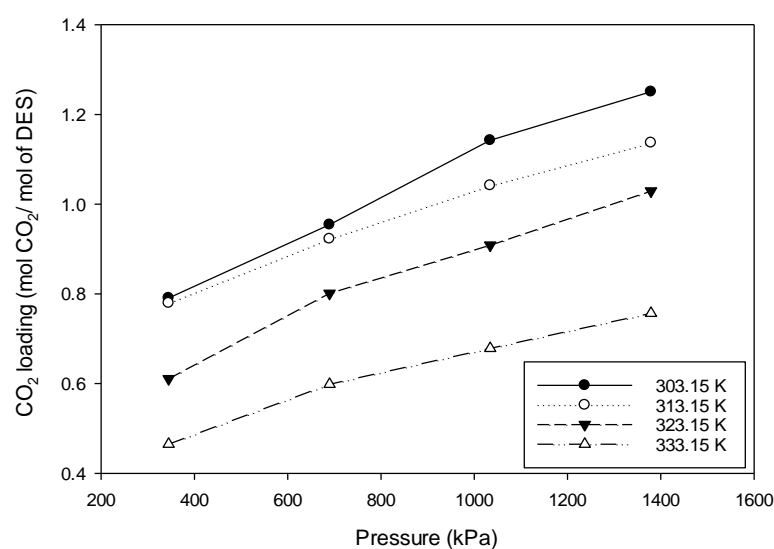
Figure 4. CO_2 absorption of (**a**) 2M ChOH:DETA−DMSO; (**b**) 2M ChOH:TETA−DMSO; (**c**) 2M ChOH:DETA-Sulfolane; (**d**) 2M ChOH:TETA−Sulfolane. at 303.15–333.15 K and various pressures.

Generally, non-aqueous organic solvents have significant advantages of low energy penalty and reduced corrosiveness as well as less amine degradation compared to aqueous solvents [27]. As reported in the literature, an amine-based non-aqueous solvent resulted in a reduction of energy consumption by up to 1.73 MJ/kg, which is 55% lower than that of an amine-based aqueous solvent [28–30]. Figure 5 shows a comparison between 2M ChOH:DETA-Sulfolane and 2M ChOH:DETA−DMSO at 313.15 K and various pressures. The results show that the 2M ChOH:DETA−DMSO mixture absorbed up to 1.137 mol CO_2/mol DES, 12.5% higher compared to 2M ChOH:DETA−Sulfolane. Similarly, Figure 5 shows a CO_2 absorption capacity of 2M ChOH:DETA and 2M ChOH:TETA mixed in sulfolane at 303.15 K and at the pressure range measured. From both observations on

solubility in non-aqueous solvents, DMSO gives a better CO_2 absorption capacity compared to sulfolane. This is due to a higher physical solubility of CO_2 in DMSO as compared to sulfolane. A similar observation was reported in the measurement of CO_2 solubility in the binary solvent of aqueous DMSO and sulfolane with MDEA, which clearly showed that the CO_2 solubility in aqueous DMSO + MDEA was higher than sulfolane + MDEA [17]. Based on these observations, the CO_2 solubility of 2M ChOH:TETA−Sulfolane reached up to 1.2507 mol CO_2/mol DES, 12.5% higher compared to 2M ChOH:DETA−Sulfolane. This is attributed to the presence of a higher number of amine moieties in the TETA polyamine carbon chain compared to DETA polyamine, which was able to react and bond more CO_2 to the molecule. A similar observation was reported in the literature, which confirmed that increasing the number of amine groups from 2 amine functionalized (EDA) to 5 amine functionalized (TEPA) drastically increased the CO_2 loading capacity [31]. Due to an increase in the number of amine active sites, the CO_2 cyclic capacity and reaction rate of amine solutions increased, allowing for the formation of numerous species, such as carbamate and bicarbonate, under equilibrium conditions [32].
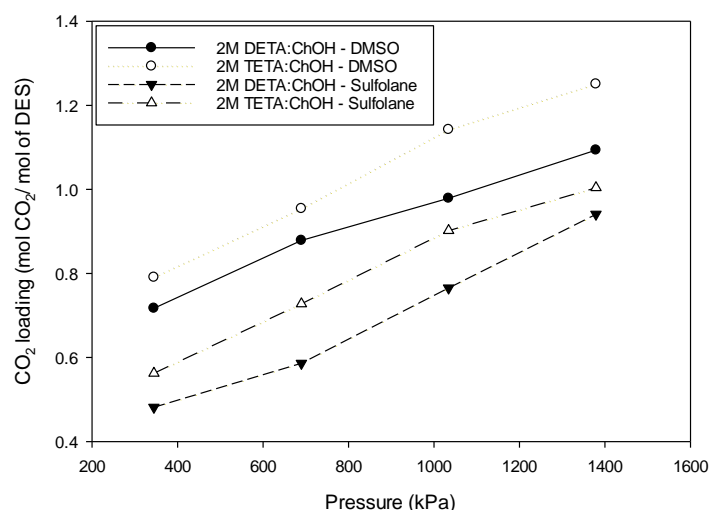
**Figure 5.** CO_2 absorption capacity of 2M DES in DMSO and sulfolane at 303.15 K and various pressures.

Furthermore, apart from 2M ChOH:DETA−DMSO, all other samples produced biphasic layers/phase separation after CO_2 absorption in a mixture with polyamine DES in the composition. Figure 6 demonstrates this phase separation. The formation of insoluble polyamine-carbamate in the non-aqueous mixture might be the source of the phase separation phenomenon. Polyamine-carbamate solubility in polar aprotic solvents such as DMSO and sulfolane is hampered by the presence of strong ionic and hydrogen bonding interactions. A similar observation was made for the CO_2 capture procedure utilizing a sulfolane combination of monoethanolamine and 1-butyl-3-methylimidazolium bis(trifluoromethylsulfonyl)imide [21]. The formation of this phase separation could contribute to more energy efficiency during the solvent regeneration step by only regenerating the CO_2-rich portion of the solution, reducing the amount of transported material to be regenerated [33].

### 3.3. Fourier Transform Infrared Analysis

Table 2 tabulates the major peaks and their assigned groups, while Figure 7a–d illustrate the FTIR spectra for 2M ChOH:TETA−DMSO, 2M ChOH:TETA−Sulfolane, 2M ChOH:DETA−DMSO and 2M ChOH:DETA−Sulfolane before and after CO_2 absorption. The presence of carbamate could be observed through the formation of the new peaks starting from 1100 to 1700 cm^{-1}. The spectra show the presence of carbonate peaks reflecting the formation of carbamate salt after absorption of CO_2, 1313, 1416, 1306, 1401 cm^{-1}, respectively. The presence of these peaks can be attributed to the nitrogen atom bonded to two imide groups, indicating the occurrence of a reaction between carbon dioxide (CO_2)

and the nitrogen atom linked to the carbonyl group (C=O) within the amide group [34]. Moreover, the establishment of a new peak formation at 1738, 1651, 1654 and 1641 cm^{-1}, respectively, is due to the skeletal vibration of NCOO$^-$. The formation of protonated amine may also contribute to the mentioned peak. It is worth mentioning that the individual amine groups present in TETA and DETA possess the potential to function as bases or participate in the formation of carbamates, encompassing monocarbamates, bicarbamates, tricarbamates, and tetracarbamates. All spectra show peaks that were found in the respective singular component; however, some peaks maybe be overlapped. An accurate assignment of all absorption bands in infrared spectra is challenging due to the extensive presence of numerous absorbing species, resulting in bands that are closely proximate, significantly broad, and often exhibiting a strong overlap.
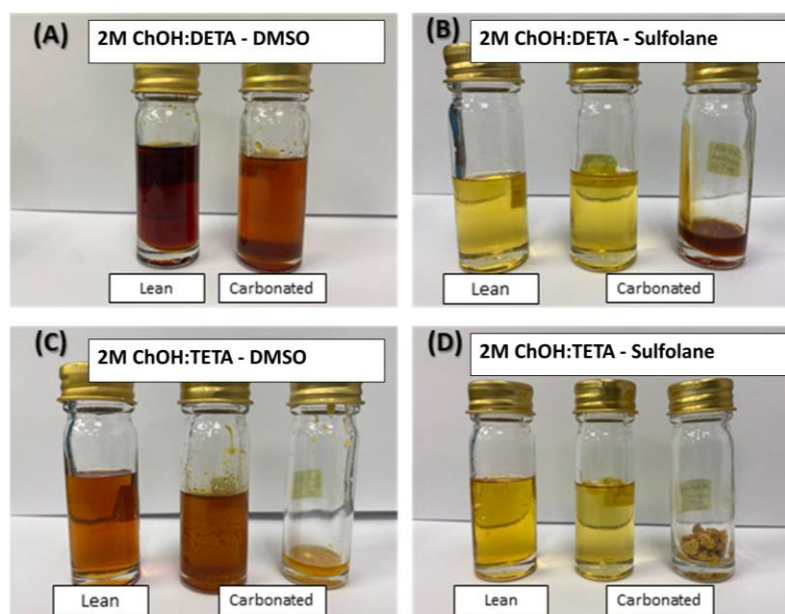
Figure 6. Phase separation observed in lean and carbonated solutions for (**A**) 2M ChOH:DETA−DMSO; (**B**) 2M ChOH:TETA−DMSO; (**C**) 2M ChOH:DETA−Sulfolane; (**D**) 2M ChOH:TETA−Sulfolane.

Figure 7. *Cont.*

2M ChOH:TETA - Sulfolane
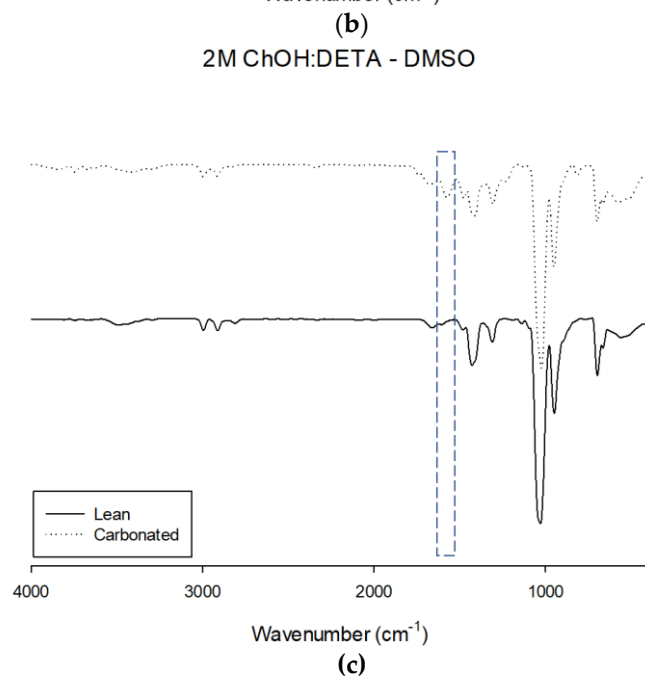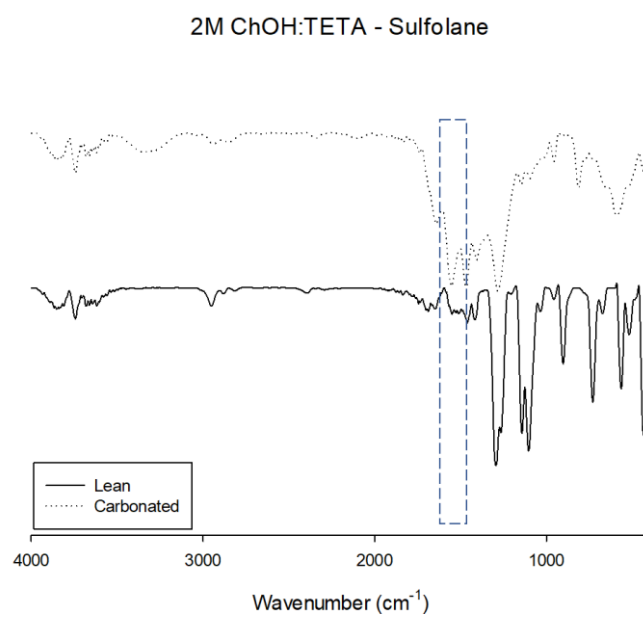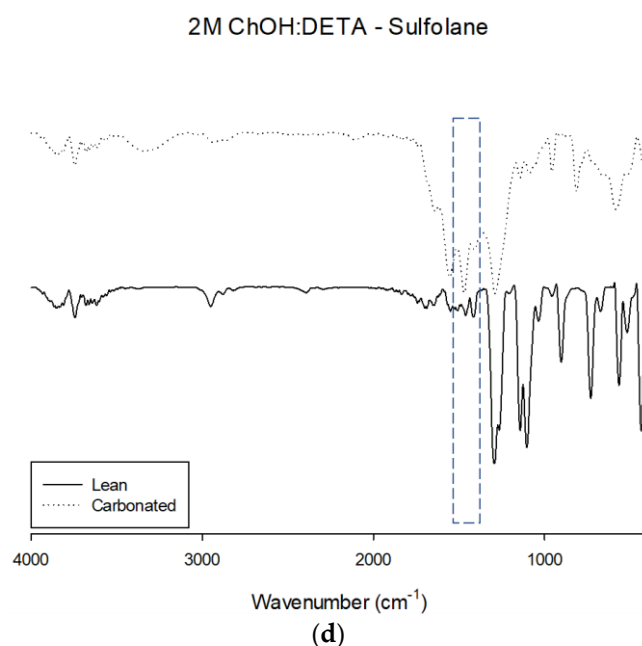

(b)

2M ChOH:DETA - DMSO

(c)
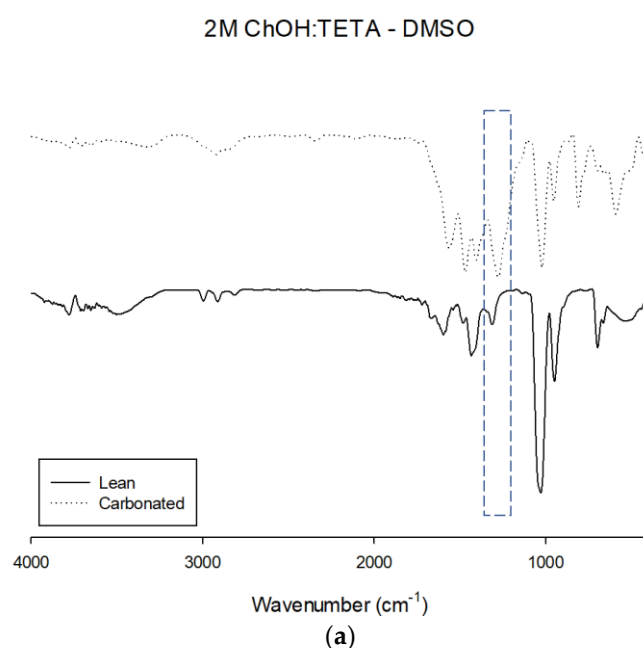
Figure 7. *Cont.*

Figure 7. FTIR spectra of lean and carbonated 2M DES non-aqueous solutions; (**a**) 2M ChOH:TETA−DMSO, (**b**) 2M ChOH:TETA−Sulfolane, (**c**) 2M ChOH:DETA−DMSO, (**d**) 2M ChOH:DETA−Sulfolane.

Table 2. FTIR peak assignment for the studied systems.

Assignment	2M ChOH:DETA-DMSO	2M ChOH:DETA-Sulfolane	2M ChOH:TETA-DMSO	2M ChOH:TETA-Sulfolane
	Frequency (cm^{-1})			
−OH, −NH stretching	3419	3337	3315	3536
−NH bending	698, 663	581	656, 699	673
−CH$_2$−OH bending	1572	1552	1562	1550
−C−N− bending	1230	1267	1276	1264
−C−O− bending	1023	-	1020	1035
Carbamates band	1306	1410	1313, 1348	1416
−CH$_2$−, −CH$_3$ stretching	1476, 1410	1469	1403, 1468	1461
stretching of NCOO−	1654	1641		1651

3.4. Comparison with Another Study

Figure 8 shows a comparison between the CO_2 loading capacity of this study and that of the work by Mohammad et al. (2019), using 2M ChOH:TETA−DMSO and 2M GLY−DMAPA, respectively, at 303.15 K. For both samples, the CO_2 loading increases with an increasing pressure, and this is mostly in agreement with other published literature. At the highest measured pressure, the results indicated that the CO_2 absorption capacity of 2M ChOH:TETA−DMSO (1.2507 mol CO_2/mol absorbent) was higher than 2M DMAPA−GLY (0.720 mol CO_2/mol absorbent) [34]. The high CO_2 loading observed in 2M ChOH:TETA−DMSO solution is mainly due to the presence of two primary and two secondary amino groups in its chemical structure, which provide an active site for capturing CO_2, making TETA a high CO_2 loading species [35]. Moreover, the increasing trend in CO_2 absorption at a high pressure is attributed to the presence of more CO_2 molecules at elevated pressures of CO_2 as well as a higher kinetic energy, which resulted in a higher probability of collisions between CO_2 molecules and 2M ChOH:TETA−DMSO.

The observed differences in solubility can be explained by the variations in the physical absorbent components, notably DMSO and glycerine.
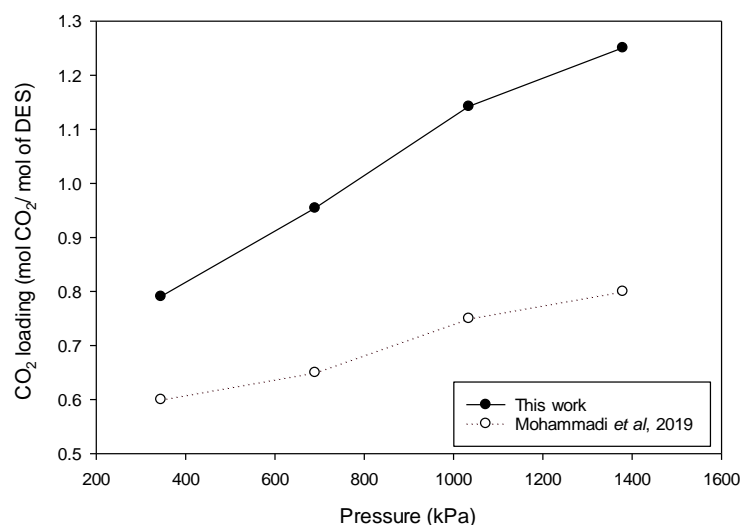
Figure 8. Comparison of the CO_2 loading capacity of polyamine non-aqueous mixture at T = 303.15 K of this work with Mohammad et al.'s works [34].

4. Conclusions

A non-aqueous mixture of choline hydroxide-based deep eutectic solvent has been developed with an enhanced CO_2 absorption capacity. The implementation of DES as a viable alternative for commercial CO_2 absorbents appears advantageous due to its cost-effectiveness resulting from the utilization of inexpensive raw materials and a straightforward synthesis process. Furthermore, the incorporation of polyamine has demonstrated a significant enhancement in its capacity to capture CO_2, with the presence of multiple amine groups in the structure. The results demonstrated that 2M ChOH:TETA−DMSO exhibits a superior CO_2 loading capacity (mol CO_2/mol DES) compared to 2M ChOH:TETA−Sulfolane, 2M ChOH:DETA−DMSO and 2M ChOH:DETA−Sulfolane. This is due to the presence of a high number of amine groups in the TETA molecule compared to DETA and a higher physical solubility of CO_2 in DMSO compared to sulfolane. We also observed that the absorption capacity increased with an increasing pressure and decreased temperature. The highest CO_2 absorption by 2M ChOH:TETA−DMSO was observed at a partial pressure of 1400 kPa at 303.15 K. Furthermore, a phase separation was observed in most of the solutions post-CO_2 absorption process. This is due to the formation of insoluble carbamate salt, which was identified through FTIR analysis. The formation of a phase separation by the CO_2-rich layer of carbamate salt could contribute to a more energy-efficient regeneration process. This is possible via selectively transporting the CO_2-rich layer, thus reducing the amount of material transported during the regeneration process. By only regenerating the CO_2-rich phase of the absorbent, the total energy required for the regeneration process could be reduced. Moreover, with the incorporation of polyamine, a higher number of CO_2 was absorbed. However, future studies are necessary to evaluate the absorbent's performance in real-world applications and to determine the optimal operating conditions.

References

1. Zubeir, L.F.; Lacroix, M.H.; Meuldijk, J.; Kroon, M.C.; Kiss, A.A. Novel pressure and temperature swing processes for CO_2 capture using low viscosity ionic liquids. *Sep. Purif. Technol.* **2018**, *204*, 314–327. [CrossRef]
2. Madejski, P.; Chmiel, K.; Subramanian, N.; Kuś, T. Methods and Techniques for CO_2 Capture: Review of Potential Solutions and Applications in Modern Energy Technologies. *Energies* **2022**, *15*, 887. [CrossRef]
3. Jiang, L.; Gonzalez-Diaz, A.; Ling-Chin, J.; Roskilly, A.P.; Smallbone, A.J. Post-combustion CO_2 capture from a natural gas combined cycle power plant using activated carbon adsorption. *Appl. Energy* **2019**, *245*, 1–15. [CrossRef]
4. Ochedi, F.O.; Yu, J.; Yu, H.; Liu, Y.; Hussain, A. Carbon dioxide capture using liquid absorption methods: A review. *Environ. Chem. Lett.* **2020**, *19*, 77–109. [CrossRef]
5. Vega, F.; Baena-Moreno, F.; Fernández, L.M.G.; Portillo, E.; Navarrete, B.; Zhang, Z. Current status of CO_2 chemical absorption research applied to CCS: Towards full deployment at industrial scale. *Appl. Energy* **2019**, *260*, 114313. [CrossRef]
6. Ünveren, E.E.; Monkul, B.Ö.; Sarıoğlan, Ş.; Karademir, N.; Alper, E. Solid amine sorbents for CO_2 capture by chemical adsorption: A review. *Petroleum* **2017**, *3*, 37–50. [CrossRef]
7. Ali, S.A.; Mulk, W.U.; Ullah, Z.; Khan, H.; Zahid, A.; Shah, M.U.H.; Shah, S.N. Recent Advances in the Synthesis, Application and Economic Feasibility of Ionic Liquids and Deep Eutectic Solvents for CO_2 Capture: A Review. *Energies* **2022**, *15*, 9098. [CrossRef]
8. Smith, E.L.; Abbott, A.P.; Ryder, K.S. Deep Eutectic Solvents (DESs) and Their Applications. *Chem. Rev.* **2014**, *114*, 11060–11082. [CrossRef]
9. Leron, R.B.; Li, M.-H. Solubility of carbon dioxide in a choline chloride–ethylene glycol based deep eutectic solvent. *Thermochim. Acta* **2013**, *551*, 14–19. [CrossRef]
10. Ali, E.; Hadj-Kali, M.K.; Mulyono, S.; Alnashef, I.; Fakeeha, A.; Mjalli, F.; Hayyan, A. Solubility of CO_2 in deep eutectic solvents: Experiments and modelling using the Peng–Robinson equation of state. *Chem. Eng. Res. Des.* **2014**, *92*, 1898–1906. [CrossRef]
11. Mahi, M.R.; Mokbel, I.; Negadi, L.; Dergal, F.; Jose, J. Experimental solubility of carbon dioxide in monoethanolamine, or diethanolamine or N-methyldiethanolamine (30 wt%) dissolved in deep eutectic solvent (choline chloride and ethylene glycol solution). *J. Mol. Liq.* **2019**, *289*, 111062. [CrossRef]
12. Mirza, N.; Mumford, K.; Wu, Y.; Mazhar, S.; Kentish, S.; Stevens, G. Improved Eutectic Based Solvents for Capturing Carbon Dioxide (CO_2). *Energy Procedia* **2017**, *114*, 827–833. [CrossRef]
13. Karlsson, H.K.; Makhool, H.; Karlsson, M.; Svensson, H. Chemical absorption of carbon dioxide in non-aqueous systems using the amine 2-amino-2-methyl-1-propanol in dimethyl sulfoxide and N-methyl-2-pyrrolidone. *Sep. Purif. Technol.* **2020**, *256*, 117789. [CrossRef]
14. Kant, V.; Jangir, B.L.; Kumar, V. Gross and histopathological effects of dimethyl sulfoxide on wound healing in rats. *Wound Med.* **2020**, *30*, 100194. [CrossRef]
15. Li, X.; Zhou, X.; Wei, J.; Fan, Y.; Liao, L.; Wang, H. Reducing the energy penalty and corrosion of carbon dioxide capture using a novel nonaqueous monoethanolamine-based biphasic solvent. *Sep. Purif. Technol.* **2021**, *265*, 118481. [CrossRef]
16. Zhou, X.; Liu, C.; Fan, Y.; Zhang, L.; Tang, S.; Mo, S.; Zhu, Y.; Zhu, Z. Energy-efficient carbon dioxide capture using a novel low-viscous secondary amine-based nonaqueous biphasic solvent: Performance, mechanism, and thermodynamics. *Energy* **2022**, *255*, 124570. [CrossRef]
17. Shirazizadeh, H.A.; Haghtalab, A. Measurement and modeling of CO_2 solubility in binary aqueous DMSO and MDEA and their ternary mixtures at different temperatures and compositions. *Fluid Phase Equilibria* **2020**, *528*, 112845. [CrossRef]
18. Wang, L.; Yu, S.; Li, Q.; Zhang, Y.; An, S.; Zhang, S. Performance of sulfolane/DETA hybrids for CO_2 absorption: Phase splitting behavior, kinetics and thermodynamics. *Appl. Energy* **2018**, *228*, 568–576. [CrossRef]
19. Liu, S.; Ling, H.; Lv, J.; Gao, H.; Na, Y.; Liang, Z. New Insights and Assessment of Primary Alkanolamine/Sulfolane Biphasic Solutions for Post-combustion CO_2 Capture: Absorption, Desorption, Phase Separation, and Technological Process. *Ind. Eng. Chem. Res.* **2019**, *58*, 20461–20471. [CrossRef]
20. Hussin, F.; Aroua, M.K.; Yusoff, R. Adsorption of CO_2 on palm shell based activated carbon modified by deep eutectic solvent: Breakthrough adsorption study. *J. Environ. Chem. Eng.* **2021**, *9*, 105333. [CrossRef]
21. Kassim, M.A.; Sairi, N.A.; Yusoff, R.; Alias, Y.; Aroua, M.K. Evaluation of 1-Butyl-3-methylimidazolium Bis(trifluoromethylsulfonyl)imide –Alkanolamine Sulfolane-Based System as Solvent for Absorption of Carbon Dioxide. *Ind. Eng. Chem. Res.* **2016**, *55*, 7992–8001. [CrossRef]

22. Jalili, A.H.; Shokouhi, M.; Samani, F.; Hosseini-Jenab, M. Measuring the solubility of CO_2 and H_2S in sulfolane and the density and viscosity of saturated liquid binary mixtures of (sulfolane + CO_2) and (sulfolane + H_2S). *J. Chem. Thermodyn.* **2015**, *85*, 13–25. [CrossRef]

23. Barzagli, F.; Peruzzini, M.; Zhang, R. Direct CO_2 capture from air with aqueous and nonaqueous diamine solutions: A comparative investigation based on 13C NMR analysis. *Carbon Capture Sci. Technol.* **2022**, *3*, 100049. [CrossRef]

24. Muchan, P.; Narku-Tetteh, J.; Saiwan, C.; Idem, R.; Supap, T. Effect of number of amine groups in aqueous polyamine solution on carbon dioxide (CO_2) capture activities. *Sep. Purif. Technol.* **2017**, *184*, 128–134. [CrossRef]

25. Tzirakis, F.; Papadopoulos, A.I.; Seferlis, P.; Tsivintzelis, I. CO_2 Solubility in diethylenetriamine (DETA) and triethylenetetramine (TETA) aqueous mixtures: Experimental investigation and correlation using the CPA equation of state. *Chem. Thermodyn. Therm. Anal.* **2021**, *3–4*, 100017. [CrossRef]

26. Luo, W.; Guo, D.; Zheng, J.; Gao, S.; Chen, J. CO_2 absorption using biphasic solvent: Blends of diethylenetriamine, sulfolane, and water. *Int. J. Greenh. Gas Control* **2016**, *53*, 141–148. [CrossRef]

27. Ping, T.; Dong, Y.; Shen, S. Energy-Efficient CO_2 Capture Using Nonaqueous Absorbents of Secondary Alkanolamines with a 2-Butoxyethanol Cosolvent. *ACS Sustain. Chem. Eng.* **2020**, *8*, 18071–18082. [CrossRef]

28. Guo, H.; Li, C.; Shi, X.; Li, H.; Shen, S. Nonaqueous amine-based absorbents for energy efficient CO_2 capture. *Appl. Energy* **2019**, *239*, 725–734. [CrossRef]

29. Barzagli, F.; Giorgi, C.; Mani, F.; Peruzzini, M. Comparative Study of CO_2 Capture by Aqueous and Nonaqueous 2-Amino-2-methyl-1-propanol Based Absorbents Carried Out by ^{13}C NMR and Enthalpy Analysis. *Ind. Eng. Chem. Res.* **2019**, *58*, 4364–4373. [CrossRef]

30. Alkhatib, I.I.; Pereira, L.M.; AlHajaj, A.; Vega, L.F. Performance of non-aqueous amine hybrid solvents mixtures for CO_2 capture: A study using a molecular-based model. *J. CO2 Util.* **2019**, *35*, 126–144. [CrossRef]

31. Wang, Z.; Fang, M.; Pan, Y.; Yan, S.; Luo, Z. Amine-based absorbents selection for CO_2 membrane vacuum regeneration technology by combined absorption–desorption analysis. *Chem. Eng. Sci.* **2013**, *93*, 238–249. [CrossRef]

32. Jung, W.; Lee, J. Thermodynamic and kinetic modeling of a novel polyamine-based solvent for energy-efficient CO_2 capture with energy analysis. *Energy* **2021**, *239*, 122347. [CrossRef]

33. Gao, G.; Jiang, W.; Li, X.; Zhao, Z.; Jiang, C.; Luo, C.; Wu, F.; Zhang, L. Novel assessment of highly efficient polyamines for post-combustion CO_2 capture: Absorption heat, reaction rate, CO_2 cyclic capacity, and phase change behavior. *Sep. Purif. Technol.* **2023**, *306*, 122615. [CrossRef]

34. Mohsin, H.M.; Shariff, A.M.; Johari, K. 3-Dimethylaminopropylamine (DMAPA) mixed with glycine (GLY) as an absorbent for carbon dioxide capture and subsequent utilization. *Sep. Purif. Technol.* **2019**, *222*, 297–308. [CrossRef]

35. Liu, F.; Jing, G.; Zhou, X.; Lv, B.; Zhou, Z. Performance and Mechanisms of Triethylene Tetramine (TETA) and 2-Amino-2-methyl-1-propanol (AMP) in Aqueous and Nonaqueous Solutions for CO_2 Capture. *ACS Sustain. Chem. Eng.* **2017**, *6*, 1352–1361. [CrossRef]